

# Serum neurofilament levels reflect outer retinal layer changes in multiple sclerosis

Caspar B. Seitz<sup>1</sup>, Falk Steffen, Muthuraman Muthuraman<sup>2</sup>, Timo Uphaus, Julia Krämer, Sven G. Meuth, Philipp Albrecht, Sergiu Groppa, Frauke Zipp, Stefan Bittner\* and Vinzenz Fleischer\*<sup>3</sup>

*Ther Adv Neurol Disord*

2021, Vol. 14: 1–14

DOI: 10.1177/  
17562864211003478

© The Author(s), 2021.  
Article reuse guidelines:  
sagepub.com/journals-  
permissions

## Abstract

**Background:** Serum neurofilament light chain (sNfL) and distinct intra-retinal layers are both promising biomarkers of neuro-axonal injury in multiple sclerosis (MS). We aimed to unravel the association of both markers in early MS, having identified that neurofilament has a distinct immunohistochemical expression pattern among intra-retinal layers.

**Methods:** Three-dimensional (3D) spectral domain macular optical coherence tomography scans and sNfL levels were investigated in 156 early MS patients (female/male: 109/47, mean age:  $33.3 \pm 9.5$  years, mean disease duration:  $2.0 \pm 3.3$  years). Out of the whole cohort, 110 patients had no history of optic neuritis (NHON) and 46 patients had a previous history of optic neuritis (HON). In addition, a subgroup of patients ( $n=38$ ) was studied longitudinally over 2 years. Support vector machine analysis was applied to test a regression model for significant changes.

**Results:** In our cohort, HON patients had a thinner outer plexiform layer (OPL) volume compared to NHON patients ( $B=-0.016$ ,  $SE=0.006$ ,  $p=0.013$ ). Higher sNfL levels were significantly associated with thinner OPL volumes in HON patients ( $B=-6.734$ ,  $SE=2.514$ ,  $p=0.011$ ). This finding was corroborated in the longitudinal subanalysis by the association of higher sNfL levels with OPL atrophy ( $B=5.974$ ,  $SE=2.420$ ,  $p=0.019$ ). sNfL levels were 75.7% accurate at predicting OPL volume in the supervised machine learning.

**Conclusions:** In summary, sNfL levels were a good predictor of future outer retinal thinning in MS. Changes within the neurofilament-rich OPL could be considered as an additional retinal marker linked to MS neurodegeneration.

**Keywords:** multiple sclerosis, neuroimmunology, optical coherence tomography, optic neuritis, serum neurofilament, translation

Received: 22 October 2020; revised manuscript accepted: 28 February 2021.

## Introduction

Monitoring the neuroinflammatory and chronic neurodegenerative component of multiple sclerosis (MS) pathology is crucial for individualized patient treatment decisions and development of new treatment paradigms. These pathological changes can be assessed by magnetic resonance imaging (MRI) of the brain, but also regionally by optical coherence tomography (OCT) of the eye. OCT is a valuable technique to study tissue alterations within the central nervous system (CNS).

The visual system offers a unique and easily accessible window into the CNS of MS patients, allowing researchers to monitor inflammatory activity within the retina and to measure neuro-axonal loss of intra-retinal layers by OCT on a microscopic scale.<sup>1,2</sup> Swelling of intra-retinal layers such as transient thickening of the inner nuclear layer (INL) and outer plexiform layer (OPL) has been associated with inflammation,<sup>3</sup> whereas atrophy of selected layers; for example, macular retinal nerve fiber layer (mRNFL) or

Correspondence to:

**Vinzenz Fleischer**  
Department of  
Neurology, Focus  
Program Translational  
Neuroscience (FTN),  
Rhine Main Neuroscience  
Network (rmn<sup>2</sup>), University  
Medical Center of the  
Johannes Gutenberg  
University Mainz,  
Langenbeckstr. 1, Mainz  
55131, Germany  
[vinzenz.fleischer@unimedizin-mainz.de](mailto:vinzenz.fleischer@unimedizin-mainz.de)

**Caspar B. Seitz**  
**Falk Steffen**  
**Muthuraman Muthuraman**  
**Timo Uphaus**  
**Sergiu Groppa**  
**Frauke Zipp**  
**Stefan Bittner**  
Department of  
Neurology, Focus  
Program Translational  
Neuroscience (FTN),  
Rhine Main Neuroscience  
Network (rmn<sup>2</sup>), University  
Medical Center of the  
Johannes Gutenberg  
University Mainz, Mainz,  
Germany

**Julia Krämer**  
Department of Neurology  
with Institute of  
Translational Neurology,  
University of Münster,  
Albert-Schweizer-Campus,  
Münster, Germany

**Sven G. Meuth**  
Department of Neurology  
with Institute of  
Translational Neurology,  
University of Münster,  
Albert-Schweizer-Campus,  
Münster, Germany

Department of Neurology,  
Medical Faculty,  
Heinrich-Heine University,  
Düsseldorf, Germany

**Philipp Albrecht**  
Department of Neurology,  
Medical Faculty,  
Heinrich-Heine University,  
Düsseldorf, Germany

\*Equally contributing  
senior authors

ganglion cell and inner plexiform layer (GCIPL) thinning, has been linked to neurodegeneration.<sup>4</sup>

The strength of the visual system as a marker of MS disease activity or progression lays in the fact that it is frequently and early affected in MS patients.<sup>5</sup> The majority of MS patients in *post mortem* studies exhibited an affected optic nerve.<sup>6,7</sup> Marked thinning of the inner retinal layers, such as mRNFL and GCIPL, driven by retrograde neuro-axonal degeneration, has been shown to correlate with poor visual outcome and the prior presence of optic neuritis (ON)<sup>8</sup> even in the case of clinically asymptomatic ON in clinically isolated syndrome (CIS).<sup>9</sup> Furthermore, due to demyelinating lesions in the optic radiation and the visual cortex, retrograde trans-synaptic changes are traceable in the retina.<sup>10</sup>

Besides this imaging marker with good spatial resolution, serum neurofilament light chain (sNfL) is an emerging fluid biomarker of neuro-axonal injury primarily independent of the underlying cause.<sup>11</sup> In the case of MS patients, sNfL is elevated during relapses<sup>12</sup> and correlates with an increase in T2-hyperintensive lesion load and new gadolinium-enhancing lesions on MRI.<sup>13</sup> Although it was found only weakly to predict the progression from CIS to relapsing–remitting multiple sclerosis (RRMS)<sup>14</sup> or the transition from RRMS to secondary progressive multiple sclerosis (SPMS),<sup>15</sup> a significant decrease in sNfL was found in MS patients after starting immunotherapeutic treatment.<sup>13,16</sup> Thus, sNfL represents a marker for acute inflammatory activity (accompanied by prompt neuronal loss) as well as (post-) inflammatory neurodegeneration over longer observation periods.<sup>17,18</sup>

Taken together, the value of sNfL in monitoring and predicting disease evolution in MS and its association with clinical and structural MRI markers of activity confirms the usefulness of this measure as a serum biomarker. Here, we aimed to unravel the association between this blood-derived biomarker and volumetric changes within the retina likewise reflecting axonal loss and neurodegeneration in MS. In a first step, we utilized an animal model to investigate the histopathological expression pattern of neurofilament in the murine retina. Then, in a clinical study, we aimed to assess whether sNfL levels in early MS patients are associated with volumetric changes of specific intra-retinal layers by using high-resolution

spectral domain OCT, enabling a detailed detection of all intra-retinal structures.

## Methods

### Participants

In total, 177 MS patients underwent OCT measurement at the outpatient clinic of the Department of Neurology, at the University Medical Center in Mainz (Germany) between October 2010 and November 2018 (Figure 1). Three patients were excluded due to differential diagnosis: neoplasm of the optic nerve, bilateral uveitis and a congenital amblyopia. Three patients were excluded because of insufficient OCT quality based on OSCAR-IB quality criteria.<sup>19,20</sup> Finally, as it would have been impossible to control for the dynamics of retinal alterations resulting from ON attacks at varying time points before the measurements,<sup>21,22</sup> 15 patients were excluded because of an ON within 6 months prior to the OCT measurement.

Therefore, 156 patients with early-stage MS were included in the final study cohort. Four of these had CIS, while the remaining 152 patients had RRMS as diagnosed according to the 2017 revised McDonald diagnostic criteria.<sup>23</sup> The mean disease duration of all patients was  $2.0 \pm 3.3$  years at study entry.

On inclusion, serum was collected to determine sNfL levels; OCT was performed  $1.9 \pm 1.7$  years after study inclusion. The cohort was divided into patients with and without a history of ON [history of optic neuritis (HON) and no history of optic neuritis (NHON), respectively] as intra-retinal volume patterns significantly differ between these groups, as previously shown.<sup>1</sup> HON was defined by medical history and patient interviews. Out of the whole cohort, 110 patients had NHON (mean time between blood draw and OCT  $1.6 \pm 1.7$  years) and 46 patients had a previous HON (mean time between blood draw and OCT  $2.4 \pm 1.7$  years). The mean time of the previous ON was  $3.9 \pm 4.1$  years prior to the OCT measurement. A subgroup of 38 patients (15 of whom had a previous HON) was studied longitudinally with OCT (baseline OCT at blood draw and follow-up OCT after  $2.1 \pm 1.4$  years). NHON and HON patients were combined in this analysis as most (although not all)<sup>1</sup> studies suggest longitudinal atrophy occurs irrespective of previous ON episodes (if their ON was more than 6 months prior to the

OCT).<sup>24</sup> Patients with an ON during the follow-up, however, were excluded.

Each patient was clinically assessed by an experienced neurologist and their Expanded Disability Status Scale (EDSS) score was determined at study entry, along with demographic data. Ocular exclusion criteria according to the OSCAR-IB criteria were ruled out based on the OCT exam and medical history.<sup>19</sup>

#### *Study protocol for OCT measurement*

The Advised Protocol for OCT Study Terminology and Elements (APOSTEL) recommendations were applied.<sup>25</sup> This included a quality control for the raw OCT scans complying with the OSCAR-IB criteria.<sup>19,20</sup> Patients with other diseases affecting the optic nerve, such as neuromyelitis optica spectrum disorder or chronic relapsing inflammatory optic neuropathy, were excluded in advance. None of the patients had a history of glaucoma, refraction anomalies ( $\geq -6$  dpt), retinopathy or other neurological disorders (besides CIS or RRMS).

#### *OCT image acquisition and scanning protocol*

An experienced operator performed OCT image acquisition following a unified standard acquisition protocol using a spectral domain (SD) OCT (Heidelberg Spectralis, Heidelberg Engineering, Germany) with Heidelberg Eye Explorer software (HEYEX, version 1.10.2.0). The measurements were acquired in a shaded room at ambient light without pupillary dilation. Intra-retinal layers of the macula were gauged by a standardized scan comprising 61 vertical or horizontal B-scans while focusing on the fovea at a scanning angle of  $30^\circ \times 25^\circ$  and a resolution of  $768 \times 496$  pixels. Automatic real time was set to nine at high speed scanning mode. Confocal scanning laser ophthalmoscopy was performed in parallel and revealed no evidence of pathology. No further fundoscopic imaging was carried out.

#### *Post-acquisition data selection and analysis*

To account for inter-eye within-patient dependencies, we calculated the mean of NHON eyes in NHON patients and the mean of HON eyes in HON patients with bilateral ON, as long as both measurements were available and of good scan quality. In HON patients with a unilateral ON,

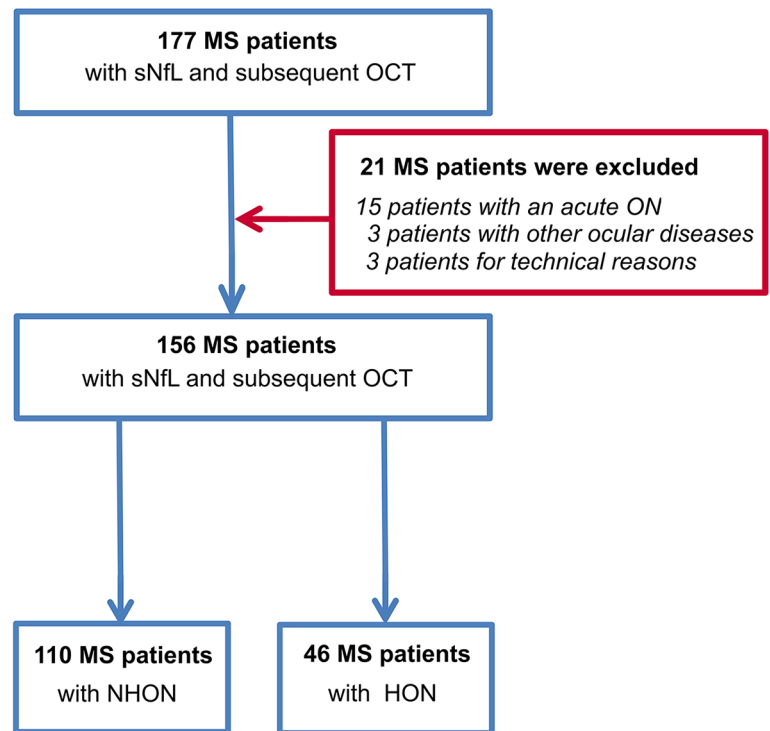


**Figure 1.** Flow chart of MS patients included in the study. HON, history of optic neuritis; MS, multiple sclerosis; NHON, no history of optic neuritis; OCT, optical coherence tomography; sNfL, serum neurofilament light chain.

we only used the OCT scan of the affected eye. Hence, the main statistical analysis was performed at a per-patient level. Detailed statistical approaches are described below.

#### *Automatic intra-retinal segmentation*

All B-scans were automatically segmented (followed by manual correction by a trained rater) using segmentation beta-software (Spectralis Viewing Module version 6.9.5.0) of the Heidelberg Eye Explorer (version 1.10.2.0) provided by the manufacturer. The segmentation lines indicate the following retinal layers: mRNFL, GCIPL, INL, OPL and outer nuclear layer (ONL), see Figure 2A. The mean volume of the individual retinal layers was computed in an area of a radius of 3.45 mm around the fovea including the fovea using the Early Treatment of Diabetic Retinopathy Study (ETDRS) grid.

#### *Serum neurofilament measurements*

Serum samples were collected by treating physicians at the University Medical Center Mainz a

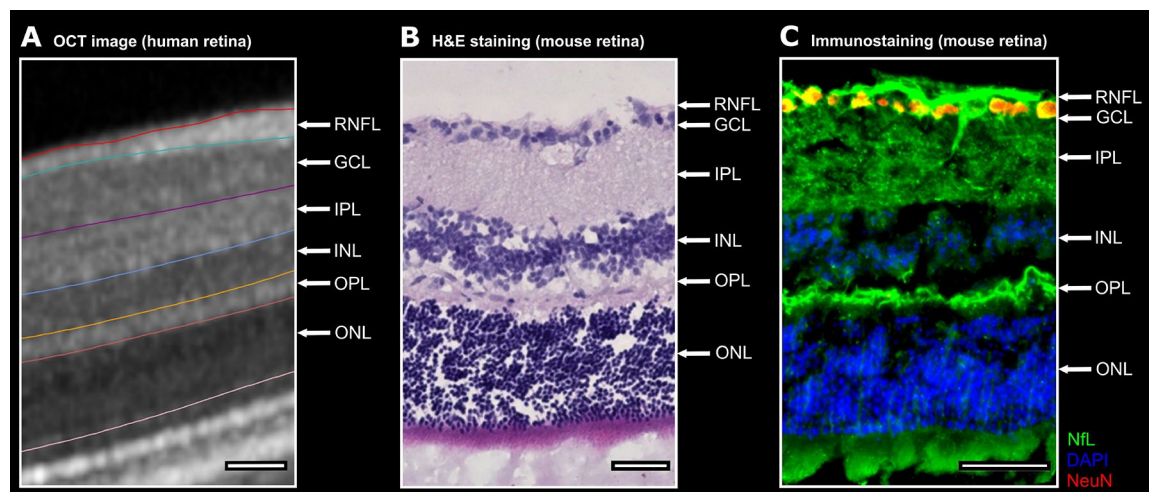


**Figure 2.** NfL and its expression pattern within the intra-retinal layers. A. One representative human OCT image with the boundaries between the intra-retinal layers is shown. B. The retinal OCT image is juxtaposed to a C57BL/6J mouse retina. The mouse retina is depicted by H&E staining. C. One representative retinal cross-section from a mouse unveils a predominant expression of neurofilament (green) in the RNFL, GCIPL and OPL. The nuclear and cytosolic antigen *NeuN* (red) is commonly used to identify neurons. For a better separation of the individual intra-retinal layers the nuclei were counterstained with DAPI (blue) a fluorescent dye strongly binding to DNA. Scale bars 50  $\mu\text{m}$ . DAPI, 4',6-Diamidin-2-phenylindol; GCIPL, ganglion cell and inner plexiform layer; H&E, hematoxylin and eosin; NeuN, neuronal nuclear antigen; NfL, neurofilament light chain; OCT, optical coherence tomography; OPL, outer plexiform layer.

mean  $11.5 \pm 25.6$  months after a relapse. Samples were processed at room temperature within 2 h. Serum samples were spun at 2000g at room temperature for 10 min, aliquoted in polypropylene tubes and stored at  $-80^{\circ}\text{C}$ . sNfL concentrations were measured in duplicate *via* single molecule array on a SiMoA HD-1 (Quanterix, USA) following the manufacturer's instructions using the NF-Light Advantage Kit (Quanterix) as previously described.<sup>26</sup> The mean intra-assay coefficient of variation (CV) of duplicate determinations for concentration was 11%. Inter-assay CV was 13% for our control sample with a mean concentration of 13.8 pg/ml. Measurements were performed a second time for the few samples in which the first run resulted in a CV above 20%. All measurements were performed in a blinded fashion with regard to diagnosis and clinical status of patients.

#### Histological stainings

To determine the immunohistopathological expression pattern of neurofilament in the retina in a preclinical mouse model, we used the retinas of 6 to 8-week-old female C57BL/6J mice (Charles River Laboratories; USA). Eyeballs were isolated from lethally anaesthetized mice after transcardial perfusion. The tissue was post-fixed,

cryoprotected and embedded; 10  $\mu\text{m}$  slices were prepared on a cryostat. The slices were incubated with appropriate dilutions of primary antibodies (chicken polyclonal anti-68 kDa neurofilament, 1:400, Abcam, UK; mouse anti-NeuN [A60], 1:1000, Merck, Germany) at  $4^{\circ}\text{C}$  overnight. Corresponding fluorochrome-conjugated secondary antibodies (goat anti-chicken 488 and goat anti-mouse 647, 1:1000, both Thermo Fisher Scientific, USA) were incubated with the slices for 3 h at room temperature. Nuclei were counterstained with 4',6-Diamidin-2-phenylindol (DAPI; 1:10,000; Thermo Fisher Scientific, USA). The control staining without the primary antibodies revealed no non-specific binding of the secondary antibodies used.

#### Statistical analysis

Statistical analysis was done using SPSS 23 software (SPSS, Chicago, IL, USA). First, the Shapiro–Wilk test was performed for the clinical and demographic variables that showed non-normality. Continuous (age and disease duration) and ordinal (EDSS) variables were compared using a Mann–Whitney *U* test. Categorical variables (sex) were compared using a Pearson's chi-square test.

To compare differences in intra-retinal volumes between NHON and HON patients we calculated statistical significance for cross-sectional analyses using a multiple linear regression model adjusting for age, sex, EDSS and disease duration.

The value of sNfL was log-transformed to achieve approximate normality. Then sNfL values were compared with the volume of intra-retinal layers by multiple linear regressions in HON as well as NHON patients adjusted for age, sex, EDSS, disease duration and relapses within 180 days of sNfL draw. In addition, sNfL was compared with atrophy of the intra-retinal layers in a longitudinal OCT setting also adjusting for age, sex, EDSS, disease duration and relapses within 180 days of sNfL draw. Results from the linear regression model are given with regression coefficient ( $B$ ) and standard error (SE).

#### *Support vector machine regression model*

The support vector machine (SVM) was applied to test for significant changes observed in the linear regression. SVM analysis is a powerful machine learning tool for classification and regression.<sup>27</sup> Here, we performed a SVM regression analysis representing a multiple regression method that can associate the observed and trained values and present the regression coefficient for the accuracy of the prediction. In this study, a data-driven regression model was implemented without explicitly stating a functional form indicating a non-parametric technique. The dependent variable was sNfL and the independent variables were OPL volume in the first model and OPL atrophy in the second model.

Briefly, the algorithm looks for an optimally separating threshold between the two datasets by maximizing the margin between the classes' closest points. The points lying on the boundaries are called support vectors, and the middle of the margin is the optimal separating threshold. In most cases, the linear separator is not ideal so a projection into a higher-dimensional space is performed where the data points effectively become linearly interrelated. Here, we have used the radial basis function kernel for this projection due to its good performance.<sup>27</sup> We used a grid search (min=1; max=10) to find the optimal input parameters, namely  $R$  (type of regression algorithm; 1–1000) and  $\gamma$  (0.25). The selection was checked by 10-fold cross-validation by taking 75% of the data

for training and 25% for testing. A soft-margin classifier of the calculated independent variables (OPL volume and OPL atrophy) was used for every parameter, and spurious correlations were weighted by a penalty constant,  $P$ . In order to optimize regression accuracy, this was calculated for every regressor. The validation scheme was used to assess whether the included independent variables (OPL volume and OPL atrophy) survived in the linear regression. For the SVM regression, we corrected for age, sex, EDSS, disease duration and relapses within 180 days of sNfL draw.

## Results

### *Retinal neurofilament expression*

To understand better the expression of neurofilament in the retina, we first looked at murine eyes. In Figure 2, H&E staining of the mouse retina (Figure 2B) can be compared to the OCT image of the human retina (Figure 2A). Within the mouse retina, we observed *ex vivo* that neurofilament has a specific expression pattern among the intra-retinal layers. Immunohistochemical staining of the retina revealed that the RNFL, GCIPL and OPL predominantly expressed neurofilament in comparison to the other layers (Figure 2C).

### *Clinical characteristics of study cohort*

An overview of the demographic and clinical data of the investigated cohort is shown in Table 1. The mean ( $\pm$ SD) age of the included 156 patients was  $33.3 \pm 9.5$  years. The mean disease duration was  $2.0 \pm 3.3$  years and the median disability (quantified with the EDSS score) was 1.0 (range: 0.0–6.0). After dividing the groups into HON and NHON patients, there was no difference in age, sex, disease duration or EDSS (all  $p$ -values  $>0.05$ ); the groups only differed in the time between blood draw and OCT measurement ( $p=0.002$ ). Clinical and demographic data of the MS patients in the longitudinal OCT subanalysis is provided in Table 2.

### *Three-dimensional OCT data comparisons*

The segmented intra-retinal layer volumes for NHON and HON patients were compared (Table 3). A lower volume of the mRNFL ( $B=-0.029$ ,  $SE=0.004$ ,  $p<0.001$ ), GCIPL ( $B=-0.121$ ,  $SE=0.018$ ,  $p<0.001$ ), as well as

**Table 1.** Clinical and demographic characteristics of early MS patients at baseline, divided into patients with (HON patients) and without (NHON patients) a history of optic neuritis.

	MS patients	NHON patients	HON patients	p-Value
Number	156	110	46	–
Age (mean ± SD)	33.3 ± 9.5 years	33.5 ± 9.9 years	32.9 ± 8.6 years	0.795 <sup>a</sup>
Disease duration (mean ± SD)	2.0 ± 3.3 years	1.6 ± 2.8 years	2.9 ± 4.2 years	0.566 <sup>a</sup>
EDSS [median (range)]	1.0 [0–6.0]	1.0 [0–6.0]	1.0 [0–3.5]	0.436 <sup>a</sup>
Sex				
Male (n/%)	47/30%	33/30%	14/30%	0.957 <sup>b</sup>
Female (n/%)	109/70%	77/70%	32/70%	
DMT				<b>0.012<sup>b</sup></b>
No DMT (n/%)	88/56%	61/55%	27/59%	
First line (n/%)	55/35%	44/40%	11/24%	
Second line (n/%)	13/8%	5/5%	8/17%	
Time between sNfL and OCT measure (mean ± SD)	1.9 ± 1.7 years	1.6 ± 1.7 years	2.4 ± 1.7 years	<b>0.002<sup>c</sup></b>
<sup>a</sup> p-Value derived from Mann–Whitney <i>U</i> test for HON versus NHON patients. <sup>b</sup> p-Value derived from Pearson's chi-square test for HON versus NHON patients. <sup>c</sup> p-Value derived from Mann–Whitney <i>U</i> test for HON versus NHON patients. DMT, disease-modifying treatment; EDSS, Expanded Disability Status Scale; HON, history of optic neuritis; MS, multiple sclerosis; n, number; NHON, no history of optic neuritis; OCT, optical coherence tomography; SD, standard deviation; sNfL, serum neurofilament light chain. a) first-line: glatiramer acetate, interferon-beta, teriflunomide, dimethyl fumarate. b) second-line: natalizumab, fingolimod, alemtuzumab. Bold values indicate statistical significance at the $p < 0.05$ level.				

lower total macular volume (TMV;  $B = -0.135$ ,  $SE = 0.030$ ,  $p < 0.001$ ) was detected in HON patients in comparison to NHON patients. Furthermore, between-group analyses based on the intra-retinal layer volumes obtained *via* automated three-dimensional (3D) segmentation revealed lower OPL volumes ( $B = -0.016$ ,  $SE = 0.006$ ,  $p = 0.013$ ) in HON patients (Table 3). INL and ONL were not significantly different between groups (all  $p$ -values  $> 0.05$ ).

#### Association of intra-retinal volumes with sNfL levels

The volumes of the intra-retinal layers measured by OCT were compared to the logarithmic value of sNfL at baseline in a linear regression model. This was done separately for HON and NHON patients due to the distinct retinal changes after an ON (Tables 4 and 5). All analyses were adjusted for age, sex, disease duration and EDSS.

A significant correlation was only seen between high sNfL levels and low OPL volume in HON patients ( $B = -6.734$ ,  $SE = 2.514$ ,  $p = 0.011$ ) (Figure 3A and Table 4). The other intra-retinal layers showed no significant correlation with sNfL levels in HON patients (all  $p$ -values  $> 0.05$ ). Moreover, no significant linear regressions were found for sNfL and OCT measures in NHON patients (all  $p$ -values  $> 0.05$ , Table 5).

#### Association of longitudinal retinal atrophy with sNfL levels

A follow-up OCT measurement was available for 38 patients so that the atrophy of the retinal layers over time could be measured (follow-up time  $2.1 \pm 1.4$  years). For the analysis of change rates, we did not distinguish between HON and NHON patients, as no eyes with ON during the observational period were included and the HON was at least 6 months before the first OCT

measurement, thus changes due to ON were expected to be negligible for these patients (see Syc *et al.*).<sup>21</sup> Baseline sNfL correlated with a significant absolute OPL atrophy between baseline and follow-up ( $B = 5.974$ ,  $SE = 2.420$ ,  $p = 0.019$ ) (Figure 3B and Table 6). There was no significant difference over time for any of the other intra-retinal layers (all  $p$ -values  $> 0.05$ ).

#### Support vector machine regression model

To assess the accuracy of sNfL levels for predicting OPL thickness and atrophy, we employed an SVM regression analysis. First, we analyzed the predictive power of sNfL for OPL thickness in HON eyes, and found an overall regression coefficient of  $-0.75$  ( $p < 0.001$ ), indicating that higher sNfL was associated with lower OPL thickness. In the SVM approach, sNfL levels were 75.7% accurate at predicting OPL volume (Figure 3A). The training and testing accuracies were 75.9% and 76.2%, respectively.

To assess the accuracy of sNfL levels for predicting OPL atrophy between baseline and follow-up, we found an overall regression coefficient of  $-0.72$  ( $p < 0.001$ ), indicating that higher sNfL was associated with increased atrophy of OPL. In the SVM approach, sNfL levels were 72.1% accurate at predicting OPL atrophy between baseline and follow-up. Training (72.5%) and testing (71.8%) accuracies are also illustrated in Figure 3B.

#### Discussion

Our first finding is that neurofilament is preferentially expressed in the RNFL, GCIPL and OPL of the murine retina. In our subsequent clinical study, we demonstrated that sNfL levels measured in early-stage MS patients are associated with a reduced volume of the OPL in HON patients after a mean of 2.4 years. Notably, the longitudinal approach revealed that sNfL levels were also associated with a concomitant decrease in OPL thickness in MS patients over a mean time of 2.1 years, suggesting the merit of sNfL for predicting post-inflammatory driven neurodegeneration. This was further corroborated by the observation that OPL was significantly thinner in HON patients compared to NHON patients. The inner retinal layers, namely the mRNFL and GCIPL, were indeed also significantly thinner in HON than NHON patients. However, there was

**Table 2.** Clinical and demographic characteristics of early MS patients at sNfL measurement in the longitudinal OCT approach.

	MS patients longitudinal
Number	38
Age (mean $\pm$ SD)	35.6 $\pm$ 9.4 years
Disease duration (mean $\pm$ SD)	2.4 $\pm$ 3.7 years
EDSS [median (range)]	2.0 (0–5.5)
Sex	
Male (n/%)	9/24%
Female (n/%)	29/76%
DMT (baseline)	
No DMT (n/%)	20/53%
First line (n/%)	15/39%
Second line (n/%)	3/8%
DMT (follow-up)	
No DMT (n/%)	10/26%
First line (n/%)	18/47%
Second line (n/%)	10/26%
Time between sNfL and 1. OCT measure (mean $\pm$ SD)	4.7 $\pm$ 5.7 months
Time between 1. and 2. OCT measure (mean $\pm$ SD)	2.1 $\pm$ 1.4 years
DMT, disease-modifying treatment; EDSS, Expanded Disability Status Scale; MS, multiple sclerosis; OCT, optical coherence tomography; SD, standard deviation; sNfL, serum neurofilament light chain.	
a) first-line: glatiramer acetate, interferon-beta, teriflunomide, dimethyl fumarate.	
b) second-line: natalizumab, fingolimod, alemtuzumab.	

unexpectedly no association between the thickness of these layers and sNfL levels in our early MS cohort. A likely reason is that while the atrophy of the inner retinal layers provides information about the previous disease activity and HON, sNfL is a marker for the current disease activity, which may differ significantly from the previous activity of disease, especially after initiation of therapy.

Two previous studies reported only a moderate increase in neurofilament in the cerebrospinal fluid (CSF) of patients with acute ON.<sup>28–30</sup> In particular, one study showed that neurofilament

**Table 3.** Comparison of the intra-retinal layers between NHON ( $n=110$ ) and HON patients at baseline ( $n=46$ ).

Intra-retinal layer volume	NHON versus HON patients				
	NHON patients (mean $\pm$ SD)	HON patients (mean $\pm$ SD)	B <sup>a</sup>	SE <sup>b</sup>	p-Value <sup>c</sup>
TMV (mm <sup>3</sup> )	3.10 $\pm$ 0.16	2.95 $\pm$ 0.19	-0.135	0.030	<0.001
mRNFL (mm <sup>3</sup> )	0.22 $\pm$ 0.02	0.18 $\pm$ 0.02	-0.029	0.004	<0.001
GCIPL (mm <sup>3</sup> )	0.79 $\pm$ 0.09	0.65 $\pm$ 0.12	-0.121	0.018	<0.001
INL (mm <sup>3</sup> )	0.36 $\pm$ 0.03	0.36 $\pm$ 0.03	0.005	0.006	0.386
OPL (mm <sup>3</sup> )	0.31 $\pm$ 0.04	0.30 $\pm$ 0.02	-0.016	0.006	<b>0.013</b>
ONL (mm <sup>3</sup> )	0.67 $\pm$ 0.07	0.68 $\pm$ 0.07	0.020	0.013	0.129

<sup>a</sup>Regression coefficient (B) derived from linear regression.  
<sup>b</sup>Standard error derived from linear regression.  
<sup>c</sup>p-Value derived from linear regression adjusted for age, sex, EDSS and disease duration.  
B, regression coefficient; EDSS, Expanded Disability Status Scale; GCIPL, ganglion cell and inner plexiform layer; HON, history of optic neuritis; INL, inner nuclear layer; mRNFL, macular retinal nerve fiber layer; NHON, no history of optic neuritis; ONL, outer nuclear layer; OPL, outer plexiform layer; SD, standard deviation; SE, standard error; TMV, total macular volume.  
Bold values indicate statistical significance at the  $p < 0.05$  level.

**Table 4.** Correlation of sNfL and intra-retinal layer volumes of HON patients ( $n=46$ ) with OCT measurement 2.4 years after sNfL draw.

Intra-retinal layer volume	Log sNfL versus intra-retinal layer volumes in HON patients			
	HON patients (mean $\pm$ SD)	B <sup>a</sup>	SE <sup>b</sup>	p-Value <sup>c</sup>
TMV (mm <sup>3</sup> )	2.95 $\pm$ 0.19	0.387	0.378	0.312
mRNFL (mm <sup>3</sup> )	0.18 $\pm$ 0.02	4.939	2.795	0.085
GCIPL (mm <sup>3</sup> )	0.65 $\pm$ 0.12	1.018	0.530	0.062
INL (mm <sup>3</sup> )	0.36 $\pm$ 0.03	-1.448	2.052	0.485
OPL (mm <sup>3</sup> )	0.30 $\pm$ 0.02	-6.734	2.514	<b>0.011</b>
ONL (mm <sup>3</sup> )	0.68 $\pm$ 0.07	0.215	1.005	0.831
sNfL (pg/ml)	16.8 $\pm$ 27.4			

<sup>a</sup>Regression coefficient (B) derived from linear regression.  
<sup>b</sup>Standard error derived from linear regression.  
<sup>c</sup>p-Value derived from linear regression adjusted for age, sex, EDSS, disease duration and relapses within 180 days of sNfL draw.  
B, regression coefficient; EDSS, Expanded Disability Status Scale; GCIPL, ganglion cell and inner plexiform layer; HON, history of optic neuritis; INL, inner nuclear layer; mRNFL, macular retinal nerve fiber layer; OCT, optical coherence tomography; ONL, outer nuclear layer; OPL, outer plexiform layer; SD, standard deviation; SE, standard error; sNfL, serum neurofilament light chain; TMV, total macular volume.  
Bold values indicate statistical significance at the  $p < 0.05$  level.

in the CSF at the time point of ON predicted RNFL and GCIPL atrophy.<sup>30</sup> Since neurofilament in the CSF has been shown to correlate well

with levels in the serum, we would expect similar results for sNfL.<sup>31</sup> In fact, sNfL has been shown to correlate with atrophy of the pRNFL.<sup>32</sup>



**Table 5.** Correlation of sNfL and intra-retinal layer volumes of NHON patients ( $n=110$ ) with OCT measurement 1.6 years after sNfL draw.

Intra-retinal layer volume	NHON patients (mean $\pm$ SD)	Log sNfL versus OCT in NHON patients		
		B <sup>a</sup>	SE <sup>b</sup>	p-Value <sup>c</sup>
TMV (mm <sup>3</sup> )	3.10 $\pm$ 0.16	0.401	0.304	0.189
mRNFL (mm <sup>3</sup> )	0.22 $\pm$ 0.02	1.016	2.203	0.646
GCIPL (mm <sup>3</sup> )	0.79 $\pm$ 0.09	0.151	0.551	0.784
INL (mm <sup>3</sup> )	0.36 $\pm$ 0.03	1.352	1.585	0.396
OPL (mm <sup>3</sup> )	0.31 $\pm$ 0.04	-0.488	1.294	0.707
ONL (mm <sup>3</sup> )	0.67 $\pm$ 0.07	1.222	0.623	0.053
sNfL (pg/ml)	19.0 $\pm$ 33.1			

<sup>a</sup>Regression coefficient (B) derived from linear regression.  
<sup>b</sup>Standard error derived from linear regression.  
<sup>c</sup>p-Value derived from linear regression adjusted for age, sex, EDSS, disease duration and relapses within 180 days of sNfL draw. B, regression coefficient; EDSS, Expanded Disability Status Scale; GCIPL, ganglion cell and inner plexiform layer; INL, inner nuclear layer; mRNFL, macular retinal nerve fiber layer; NHON, no history of optic neuritis; OCT, optical coherence tomography; ONL, outer nuclear layer; OPL, outer plexiform layer; SD, standard deviation; SE, standard error; sNfL, serum neurofilament light chain; TMV, total macular volume.

Although the retina is devoid of myelin,<sup>33</sup> the involvement of the retina in MS pathology is much more widespread than changes of the RNFL suggest. In particular, histopathological studies show widespread inflammatory involvement not only of the retinal ganglion cells but also in the INL with infiltration of different immune cells as well as enhanced perivascular involvement.<sup>34</sup> In OCT, swelling of the INL and OPL were linked to the formation of microcystic macular edema (MME), which has been shown to correlate with disease activity and EDSS progression,<sup>3</sup> reflecting inflammatory activity and secondary neurodegeneration. Interestingly, although not specific for MS, the formation of MME is more likely to happen after ON.<sup>35</sup> Indeed, INL and OPL thickness increase has been reported at 4 months after ON in the affected eye.<sup>36</sup> Conversely, a decrease in OPL and INL is verifiable in patients in the progressive phase of the disease.<sup>37,38</sup> Taken together, the INL demonstrates a complex spectrum of abnormalities in MS, including microcystic pathology, increased thickness in association with inflammatory activity and atrophy in the later disease stages. These findings suggest that the changes within the INL appear to be non-uniform throughout the disease course.<sup>3,39-42</sup> This might also be true for

OPL alterations. Thus, the observed decrease in OPL in HON patients in our study possibly reflects secondary neurodegeneration due to earlier inflammatory disease activity and this is mirrored by high sNfL levels.

In animal models, neurofilament in rabbits has been shown to be especially abundant in the OPL compared with other retinal layers.<sup>43</sup> Moreover, our initial 'kick-off' experiment revealed that neurofilament is not homogeneously expressed among the retinal layers and that in particular RNFL and GCIPL, but also OPL, contain much of the neuronal cytoskeleton neurofilament. Hence, OPL degeneration could have preferentially contributed to higher sNfL levels. However, caution has to be exercised when translating or comparing murine observations to humans as we have done in our initial experiment. Even though the anatomy of murine and primate eyes shares a fundamental plan,<sup>44</sup> slight variations exist to satisfy unique requirements in visual function in each species.<sup>45,46</sup> This fact could also explain a lack of association between sNfL, mRNFL and GCIPL, all of them expressing neurofilament in our murine retina in the immunohistochemistry providing qualitative data (Figure 2C).

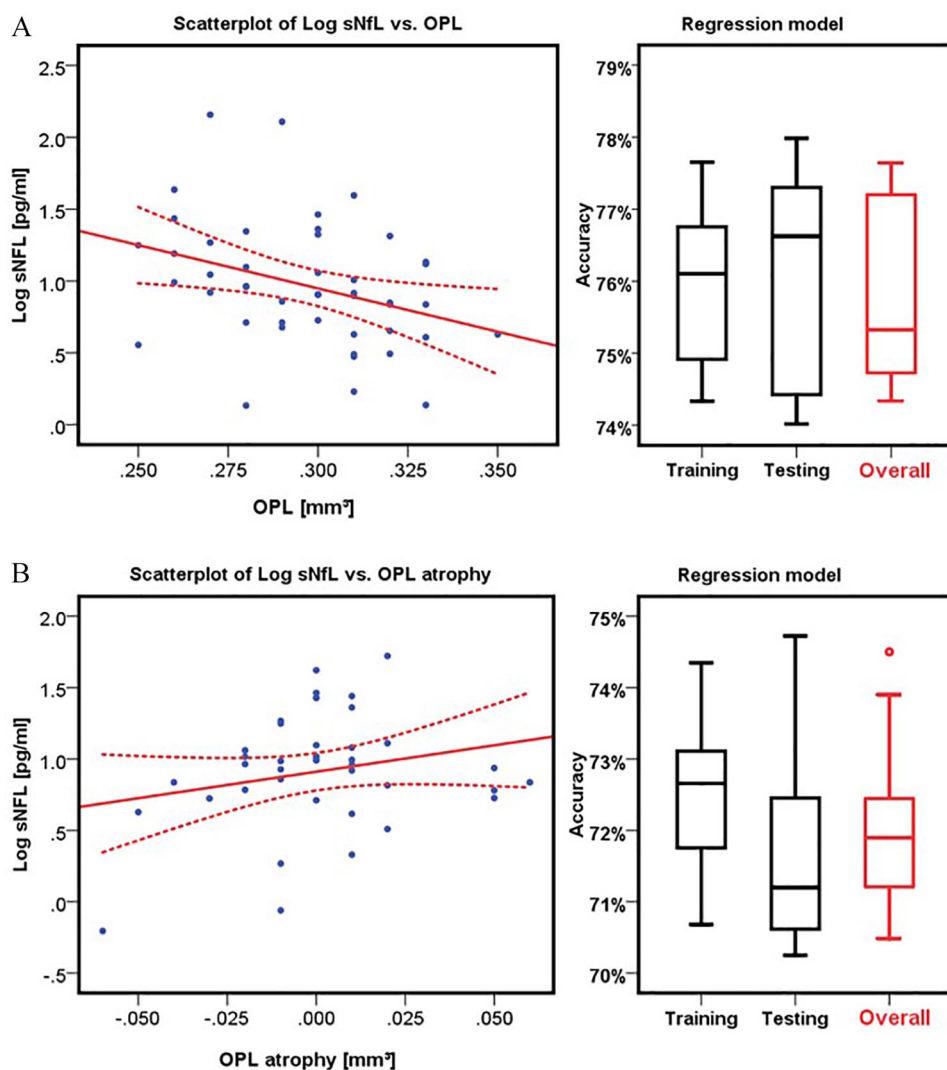


**Figure 3.** sNfL level predicts OPL thickness and atrophy in MS patients. Scatterplot for Log of sNfL and A. OPL volume and B. OPL atrophy. A. OCT was measured at a mean of 2.4 years after sNfL. The sNfL/OPL regression model was calculated to determine the accuracy of OPL thickness prediction by sNfL levels. B. OCT was measured after a mean of 0.4 years after sNfL sampling with a mean OCT follow-up of 2.1 years. The sNfL/OPL regression model was calculated to determine the accuracy of OPL atrophy prediction by sNfL levels. Log, logarithmic value; OPL, outer plexiform layer; OCT, optical coherence tomography; sNfL, serum neurofilament light chain.

Given the positive finding for a layer that has not been designated in many studies as the primary layer of interest (as opposed to the RNFL or GCIPL) and has not been investigated in association with sNfL so far, we acknowledge the exploratory nature of our study. Indeed, the only two studies on sNfL and OCT measures up to now have not investigated the OPL at all.<sup>47,48</sup>

To our knowledge, data of isolated macular OPL measures are scarce. In some studies, the OPL is roughly merged and measured together with the

INL or ONL, so data on isolated OPL changes are reserved for studies with high-contrast OCT and high spatial resolution as well as advanced analysis algorithms. Balk *et al.* reported a thinner peripapillary OPL in HON compared to NHON eyes,<sup>49</sup> although the reported changes were relatively small. However, these findings support our conclusion that changes in the OPL might primarily reflect ‘post optic neuritis’ retinal damage. Notably, the relationship between sNfL levels and OPL volumes observed in our study was not only detected in the cross-sectional approach but

**Table 6.** Correlation of sNfL at baseline and atrophy of the intra-retinal layer volumes between baseline and follow-up (mean 2.1 years) ( $n=38$ ).

Intra-retinal layer volume atrophy	MS patients (mean $\pm$ SD)	Log sNfL versus atrophy of retinal layers		
		B <sup>a</sup>	SE <sup>b</sup>	p-Value <sup>c</sup>
TMV (mm <sup>3</sup> )	-0.0016 $\pm$ 0.0520	-0.982	1.355	0.474
mRNFL (mm <sup>3</sup> )	0.0029 $\pm$ 0.0109	-9.825	6.073	0.116
GCIPL (mm <sup>3</sup> )	0.0024 $\pm$ 0.0220	-4.499	2.933	0.135
INL (mm <sup>3</sup> )	-0.0013 $\pm$ 0.0114	5.038	6.734	0.460
OPL (mm <sup>3</sup> )	0.0011 $\pm$ 0.0257	5.974	2.420	<b>0.019</b>
ONL (mm <sup>3</sup> )	-0.0026 $\pm$ 0.00254	-5.098	2.697	0.068
sNfL (pg/ml)	11.9 $\pm$ 11.1			

<sup>a</sup>Regression coefficient (B) derived from linear regression.  
<sup>b</sup>Standard error derived from linear regression.  
<sup>c</sup>p-Value derived from linear regression adjusted for age, sex, EDSS, disease duration and relapses within 180 days of sNfL draw. B, regression coefficient; EDSS, Expanded Disability Status Scale; GCIPL, ganglion cell and inner plexiform layer; INL, inner nuclear layer; mRNFL, macular retinal nerve fiber layer; MS, multiple sclerosis; ONL, outer nuclear layer; OPL, outer plexiform layer; SD, standard deviation; SE, standard error; sNfL, serum neurofilament light chain; TMV, total macular volume.  
 Bold values indicate statistical significance at the  $p < 0.05$  level.

was also reproducible in the longitudinal study. In our supervised learning model, this relationship achieved a moderate accuracy of sNfL levels for predicting OPL thickness and atrophy, respectively. However, the moderate accuracy also implies that there are certainly additional factors (beyond sNfL and the included covariates) driving OPL atrophy.

Our study has some limitations. In the cross-sectional cohort, time between sNfL sampling and subsequent OCT was different between HON and NHON patients. Moreover, the sNfL measurements at single time points can be subject to fluctuations and are therefore suboptimal due to lack of intra-individual reproduction.<sup>13</sup> In particular, studies are needed clearly to identify variables independent of disease-related factors that modify sNfL levels.<sup>50</sup> Furthermore, data were collected as part of the clinical routine in patients with various immunotherapeutic agents. These therapeutics and – even more so – changes to the therapeutic regimen and clinical relapses within the study (other than ON) were an unavoidable consequence of the real-world setting and may have had a significant influence on disease activity and hence on both the retina and sNfL levels.<sup>39</sup>

Taken together, our 3D OCT data in early MS revealed that, besides RNFL and GCIPL, OPL thinning discriminated between patients with and without a HON. Most notably, lower volume as well as increased atrophy of the neurofilament-rich OPL over time correlated with elevated sNfL levels. The fact that sNfL levels can predict OPL thinning in patients with HON strengthens its value as a liquid biomarker of inflammation-driven neuro-axonal damage. Furthermore, considering that advances in OCT techniques now offer excellent spatial resolution, changes within the OPL may be considered as a potential additional retinal marker for MS-associated or ON-associated neurodegeneration.

### Acknowledgements

The authors would like to thank Rosalind Gilchrist and Cheryl Ernest for proofreading the manuscript.

### Author contributions

CBS collected, analyzed and interpreted the data and wrote the manuscript. FS, TU and JK collected the data and critically revised the manuscript. MM performed statistical analyses. PA critically revised the manuscript. SG and SGM helped to conceptualize the study and

interpreted the data. SB, FZ and VF designed the project, were responsible for the concept, generated funding, organized patient recruitment, provided clinical information and wrote the manuscript.

#### Conflict of interest statement

The authors declare that there is no conflict of interest.

#### Funding

The authors disclosed receipt of the following financial support for the research, authorship, and/or publication of this article: This study was funded by the German Ministry for Education and Research (BMBF) German Competence Network Multiple Sclerosis (KKNMS) and the German Research Foundation (DFG) CRC-TR 128 to TU, MM, SG, FZ, SGM, SB and VF.

#### Consent for publication

Not applicable.

#### Data availability

The datasets analysed during this study are available from the corresponding author on request due to privacy/ethical restrictions.


#### Ethics approval and consent to participate

This study was approved by the local ethics committees at the University Medical Center in Mainz in Germany [approval number: 837.043.14 (9282)] and performed in accordance with the Declaration of Helsinki. All participants gave their written informed consent.

The animal work for the initial experiment was approved by the institutional animal care committee and appropriate state committees for animal welfare. The animal procedures were performed in accordance with the European Union normative for care and use of experimental animals and the German animal protection law.

#### ORCID iDs

Caspar B. Seitz  <https://orcid.org/0000-0002-3086-9730>

Muthuraman Muthuraman  <https://orcid.org/0000-0001-6158-2663>

Vinzenz Fleischer  <https://orcid.org/0000-0002-3293-5121>

#### References

1. Seitz CB, Droby A, Zaubitzer L, *et al.* Discriminative power of intra-retinal layers in early multiple sclerosis using 3D OCT imaging. *J Neurol* 2018; 265: 2284–2294.
2. Droby A, Panagoulas M, Albrecht P, *et al.* A novel automated segmentation method for retinal layers in OCT images proves retinal degeneration after optic neuritis. *Br J Ophthalmol* 2016; 100: 484–490.
3. Saidha S, Sotirchos ES, Ibrahim MA, *et al.* Microcystic macular oedema, thickness of the inner nuclear layer of the retina, and disease characteristics in multiple sclerosis: a retrospective study. *Lancet Neurol* 2012; 11: 963–972.
4. Petzold A, Balcer LJ, Calabresi PA, *et al.* Retinal layer segmentation in multiple sclerosis: a systematic review and meta-analysis. *Lancet Neurol* 2017; 16: 797–812.
5. Shams PN and Plant GT. Optic neuritis: a review. *Int MS J* 2009; 16: 82–89.
6. Ikuta F and Zimmerman HM. Distribution of plaques in seventy autopsy cases of multiple sclerosis in the United States. *Neurology* 1976; 26: 26–28.
7. Mogensen PH. Histopathology of anterior parts of the optic pathway in patients with multiple sclerosis. *Acta Ophthalmol* 1990; 68: 218–220.
8. Sanchez-Dalmau B, Martinez-Lapiscina EH, Torres-Torres R, *et al.* Early retinal atrophy predicts long-term visual impairment after acute optic neuritis. *Mult Scler* 2018; 24: 1196–1204.
9. London F, Zephir H, Drumez E, *et al.* Optical coherence tomography: a window to the optic nerve in clinically isolated syndrome. *Brain* 2019; 142: 903–915.
10. Sinnecker T, Oberwahrenbrock T, Metz I, *et al.* Optic radiation damage in multiple sclerosis is associated with visual dysfunction and retinal thinning – an ultrahigh-field MR pilot study. *Eur Radiol* 2015; 25: 122–131.
11. Gentil BJ, Tibshirani M and Durham HD. Neurofilament dynamics and involvement in neurological disorders. *Cell Tissue Res* 2015; 360: 609–620.
12. Malmestrom C, Haghighi S, Rosengren L, *et al.* Neurofilament light protein and glial fibrillary acidic protein as biological markers in MS. *Neurology* 2003; 61: 1720–1725.
13. Kuhle J, Kropshofer H, Haering DA, *et al.* Blood neurofilament light chain as a biomarker of MS

- disease activity and treatment response. *Neurology* 2019; 92: e1007–e1015.
14. Arrambide G, Espejo C, Eixarch H, *et al.* Neurofilament light chain level is a weak risk factor for the development of MS. *Neurology* 2016; 87: 1076–1084.
  15. Salzer J, Svenningsson A and Sundstrom P. Neurofilament light as a prognostic marker in multiple sclerosis. *Mult Scler* 2010; 16: 287–292.
  16. Siller N, Kuhle J, Muthuraman M, *et al.* Serum neurofilament light chain is a biomarker of acute and chronic neuronal damage in early multiple sclerosis. *Mult Scler* 2019; 25: 678–686.
  17. Disanto G, Barro C, Benkert P, *et al.* Serum neurofilament light: a biomarker of neuronal damage in multiple sclerosis. *Ann Neurol* 2017; 81: 857–870.
  18. Chitnis T, Gonzalez C, Healy BC, *et al.* Neurofilament light chain serum levels correlate with 10-year MRI outcomes in multiple sclerosis. *Ann Clin Transl Neurol* 2018; 5: 1478–1491.
  19. Tewarie P, Balk L, Costello F, *et al.* The OSCAR-IB consensus criteria for retinal OCT quality assessment. *PLoS One* 2012; 7: e34823.
  20. Schippling S, Balk LJ, Costello F, *et al.* Quality control for retinal OCT in multiple sclerosis: validation of the OSCAR-IB criteria. *Mult Scler* 2015; 21: 163–170.
  21. Syc SB, Saidha S, Newsome SD, *et al.* Optical coherence tomography segmentation reveals ganglion cell layer pathology after optic neuritis. *Brain* 2012; 135: 521–533.
  22. Gabilondo I, Martinez-Lapiscina EH, Fraga-Pumar E, *et al.* Dynamics of retinal injury after acute optic neuritis. *Ann Neurol* 2015; 77: 517–528.
  23. Thompson AJ, Banwell BL, Barkhof F, *et al.* Diagnosis of multiple sclerosis: 2017 revisions of the McDonald criteria. *Lancet Neurol* 2018; 17: 162–173.
  24. Balk LJ, Cruz-Herranz A, Albrecht P, *et al.* Timing of retinal neuronal and axonal loss in MS: a longitudinal OCT study. *J Neurol* 2016; 263: 1323–1331.
  25. Cruz-Herranz A, Balk LJ, Oberwahrenbrock T, *et al.* The APOSTEL recommendations for reporting quantitative optical coherence tomography studies. *Neurology* 2016; 86: 2303–2309.
  26. Birkner K, Loos J, Gollan R, *et al.* Neuronal ICAM-5 plays a neuroprotective role in progressive neurodegeneration. *Front Neurol* 2019; 10: 205.
  27. Cortes C and Vapnik V. Support-vector networks. *Mach Learn* 1995; 20: 273–297.
  28. Tejada-Velarde A, Costa-Frossard L, Sainz de la Maza S, *et al.* Clinical usefulness of prognostic biomarkers in optic neuritis. *Eur J Neurol* 2018; 25: 614–618.
  29. Olesen MN, Soelberg K, Debrabant B, *et al.* Cerebrospinal fluid biomarkers for predicting development of multiple sclerosis in acute optic neuritis: a population-based prospective cohort study. *J Neuroinflamm* 2019; 16: 59.
  30. Modvig S, Degn M, Sander B, *et al.* Cerebrospinal fluid neurofilament light chain levels predict visual outcome after optic neuritis. *Mult Scler* 2016; 22: 590–598.
  31. Khalil M, Teunissen CE, Otto M, *et al.* Neurofilaments as biomarkers in neurological disorders. *Nat Rev Neurol* 2018; 14: 577–589.
  32. Bsteh G, Berek K, Hegen H, *et al.* Serum neurofilament levels correlate with retinal nerve fiber layer thinning in multiple sclerosis. *Mult Scler* 2019; 26: 1682–1690.
  33. Straatsma BR, Foos RY, Heckenlively JR, *et al.* Myelinated retinal nerve fibers. *Am J Ophthalmol* 1981; 91: 25–38.
  34. Green AJ, McQuaid S, Hauser SL, *et al.* Ocular pathology in multiple sclerosis: retinal atrophy and inflammation irrespective of disease duration. *Brain* 2010; 133: 1591–1601.
  35. Kaufhold F, Zimmermann H, Schneider E, *et al.* Optic neuritis is associated with inner nuclear layer thickening and microcystic macular edema independently of multiple sclerosis. *PLoS One* 2013; 8: e71145.
  36. Al-Louzi OA, Bhargava P, Newsome SD, *et al.* Outer retinal changes following acute optic neuritis. *Mult Scler* 2016; 22: 362–372.
  37. Behbehani R, Abu Al-Hassan A, Al-Salahat A, *et al.* Optical coherence tomography segmentation analysis in relapsing remitting versus progressive multiple sclerosis. *PLoS One* 2017; 12: e0172120.
  38. Cellerino M, Cordano C, Boffa G, *et al.* Relationship between retinal inner nuclear layer, age, and disease activity in progressive MS. *Neurol Neuroimmunol Neuroinflamm* 2019; 6: e596.
  39. Knier B, Schmidt P, Aly L, *et al.* Retinal inner nuclear layer volume reflects response to immunotherapy in multiple sclerosis. *Brain* 2016; 139: 2855–2863.
  40. Sotirchos ES, Calabresi PA and Saidha S. Reply to “Retinal INL thickness in multiple sclerosis:

- a mere marker of neurodegeneration?" *Ann Neurol* 2021; 89: 193–194.
41. Sotirchos ES, Gonzalez Caldito N, Filippatou A, *et al.* Progressive multiple sclerosis is associated with faster and specific retinal layer atrophy. *Ann Neurol* 2020; 87: 885–896.
42. Cordano C, Yiu HH, Oertel FC, *et al.* Retinal INL thickness in multiple sclerosis: a mere marker of neurodegeneration? *Ann Neurol* 2021; 89: 193–194.
43. Volgyi B and Bloomfield SA. Axonal neurofilament-H immunolabeling in the rabbit retina. *J Comp Neurol* 2002; 453: 269–279.
44. Hoon M, Okawa H, Della Santina L, *et al.* Functional architecture of the retina: development and disease. *Prog Retin Eye Res* 2014; 42: 44–84.
45. Dacey DM. Primate retina: cell types, circuits and color opponency. *Prog Retin Eye Res* 1999; 18: 737–763.
46. Peichl L and González-Soriano J. Morphological types of horizontal cell in rodent retinae: a comparison of rat, mouse, gerbil, and guinea pig. *Vis Neurosci* 1994; 11: 501–517.
47. Tavazzi E, Jakimovski D, Kuhle J, *et al.* Serum neurofilament light chain and optical coherence tomography measures in MS A longitudinal study. *Neurol Neuroimmunol* 2020; 7: e737.
48. Balk LJ, Coric D, Knier B, *et al.* Retinal inner nuclear layer volume: a potential new outcome measure for optic neuritis treatment trials in MS. *Mult Scler J* 2017; 23: 271–273.
49. Balk LJ, Twisk JW, Steenwijk MD, *et al.* A dam for retrograde axonal degeneration in multiple sclerosis? *J Neurol Neurosurg Psychiatry* 2014; 85: 782–789.
50. Bridel C, Verberk IMW, Heijst JJA, *et al.* Variations in consecutive serum neurofilament light levels in healthy controls and multiple sclerosis patients. *Mult Scler Relat Disord* 2020; 47: 102666.